Supplementary Appendix to
Real-Time Density Nowcasts of U.S. Inflation: A Model-Combination Approach*

Edward S. Knotek II
Federal Reserve Bank of Cleveland

Saeed Zaman
Federal Reserve Bank of Cleveland
University of Strathclyde, UK

October 20, 2020

A.1. Description of Mixed-Frequency Models and Simulation Procedures

A.1.1. MIDAS Model

Following Knotek and Zaman (2017, KZ), a general representation of an ADL-MIDAS model with leads takes the following form,

$$\pi_{t+h} = \alpha_{(h)} + \sum_{J=0}^{P(M)-1} \chi_{j+1,(h)}\ \pi_{t-j} + \sum_{J=0}^{P(M)-1} \gamma_{j+1,(h)}\ Z_{t-j} + \beta_h \sum_{J=0}^{P(HF)-1} \omega_{P(HF)-j}\left(\theta_{(h)}^{HF}\right) X_{P(HF)-j,t+1}^{HF} + e_{t+h} \quad (1)$$

where *Z* refers to other monthly variables; *P*(*M*) refers to the number of lags of the monthly regressors (we set to 1); and *P*(*HF*) refers to the number of high-frequency observations, $X_{1,t+1}^{HF},\ldots, X_{P(HF),t+1}^{HF}$ in month t+1 (i.e., the target nowcast month). The notation (h) indicates that the coefficients are independently estimated for each forecast horizon (h). In nowcasting monthly inflation, *h* will range from 1 to 2, whereas in nowcasting quarterly inflation, *h* will range from 1 to 4. An assumption of $\sum_{J=0}^{P(HF)-1} \omega_{P(HF)-j}\left(\theta_{(h)}^{HF}\right) = 1$ helps identify β_h.

Density construction: Drawing errors from the normal distribution

Let *T* be the total number of observations (i.e., the length of the estimation window).

1. For *h*=1,..,4

---

* The views expressed herein are those of the authors and do not necessarily represent the views of the Federal Reserve Bank of Cleveland or the Federal Reserve System.

2. Estimate the model specified in equation (1) using nonlinear least squares to obtain the parameter estimates $\hat{\alpha}_{(h)}, \hat{\chi}_{(h)}, \hat{\gamma}_{(h)}, \hat{\beta}_{(h)}(\hat{\theta}_{(h)})$
3. Based on the estimates in the previous step, compute the sequence of residuals $\hat{e}_{t+h}$
4. For d=1,….,D
   a. Sample e^*_{t+h} from the empirical distribution of $e_{t+h} \sim N(0, var(\ddot{e_{t+h}}))$, where $\ddot{e_{t+h}} = \left(\frac{T}{T-k}\right)^{0.5} \hat{e}_{t+h}$ and k is the number of regressors in eq. (1).
   b. Generate a simulated series π^*_{t+h} using
   $\pi^{*\,(d)}_{t+h} = \hat{\alpha}_{(h)} + \sum_{J=0}^{P(M)-1} \hat{\chi}_{j+1,(h)}\ \pi_{t-j} + \sum_{J=0}^{P(M)-1} \hat{\gamma}_{j+1,(h)}\ Z_{t-j} + \hat{\beta}_{(h)} \sum_{J=0}^{P(HF)-1} \omega_{P(HF)-j}\left(\hat{\theta}^{HF}_{(h)}\right) X^{HF}_{P(HF)-j,t+1} + e^*_{t+h}$
   c. REPEAT
5. The empirical distribution $\{\pi^*_{t+h}\}_{d=1}^{D}$ constitutes the estimate of the density nowcast corresponding to the forecast horizon, h

Note that, in step 4a above, the draws are obtained from a distribution of modified residuals because the variance of the modified residuals is a better estimate of the true variance of the least squares estimate of the error term e_{t+h} in equation (1). To further explain why this is the case, recall that the variance of the residuals $\hat{e}_{t+h}$ is the sum of the squared residuals divided by T, whereas the variance of the least squares estimate should be divided by $T-k$, where k is the number of regressors in the regression. Therefore, the original series of residuals are rescaled to correct the variance (see Davidson and MacKinnon, 2006).

This simple procedure accounts for shock uncertainty only; i.e., it does not account for the parameter uncertainty. However, in preliminary exercises, the difference in the density accuracy between this procedure and a bootstrapping procedure that also takes into account parameter uncertainty was very small.

A.1.2. DFM Model

Our implementation of the mixed-frequency DFM follows Modugno (2013) and KZ. The dynamic factor model takes the general form:

$$y_t = Cf_t + \varepsilon_t,\ \ \varepsilon_t \sim N(0,\Sigma) \tag{2}$$

where t refers to the trading-day frequency, y_t is a vector of observations, C is a block diagonal matrix of factor loadings, ε_t is a vector of idiosyncratic components, and f_t is a vector of latent common factors following VAR dynamics:

$$Bf_t = A(L) f_{t-1} + u_t,\ u_t \sim N(0,Q)\,, \tag{3}$$

where B and $A(L)$ are matrices governing factor dynamics, some of which may be time-varying, and u_t is a vector of residuals.

With monthly, weekly, and daily data, $y_t = [y_t^M, y_t^W, y_t^D]'$, we have three corresponding factors, $f_t = [f_t^M, f_t^W, f_t^D]'$, each of dimension $r\times 1$. The monthly factor(s) f_t^M and the weekly factor(s) f_t^W are a function of the daily factor(s) f_t^D. Thus equations (2) and (3) can be written as:

$$\begin{bmatrix} y_t^M \\ y_t^W \\ y_t^D \end{bmatrix} = \begin{bmatrix} C_M & 0 & 0 \\ 0 & C_W & 0 \\ 0 & 0 & C_D \end{bmatrix} \begin{bmatrix} f_t^M \\ f_t^W \\ f_t^D \end{bmatrix} + \begin{bmatrix} \varepsilon_t^M \\ \varepsilon_t^W \\ \varepsilon_t^D \end{bmatrix} \tag{4}$$

and

$$\begin{bmatrix} 1 & 0 & -1 \\ 0 & 1 & -1 \\ 0 & 0 & 1 \end{bmatrix} \begin{bmatrix} f_t^M \\ f_t^W \\ f_t^D \end{bmatrix} = \begin{bmatrix} \Theta_t^M & 0 & 0 \\ 0 & \Theta_t^W & 0 \\ 0 & 0 & A_D \end{bmatrix} \begin{bmatrix} f_{t-1}^M \\ f_{t-1}^W \\ f_{t-1}^D \end{bmatrix} + \begin{bmatrix} 0 \\ 0 \\ u_t^D \end{bmatrix} \tag{5}$$

The matrices C_M, C_W, and C_D are the loadings for the monthly, weekly, and daily variables. Θ_t^M and Θ_t^W are time-varying coefficients: Θ_t^M is equal to zero the day after the release of the monthly data and is equal to one elsewhere; similarly, Θ_t^W is equal to zero the day after the release of the weekly data and is equal to one elsewhere.

Assuming that the monthly variables and weekly variables in our system at any time t represent a stock (i.e., a snapshot), accordingly the monthly first difference (or growth rate) and weekly first difference (or growth rate) of those variables can be formed by summing up their respective daily first differences (or growth rates).

To produce forecasts far into the future, the daily factors are forecast via the transition equation (5) and are translated to daily nowcasts and aggregated to weekly and monthly nowcasts via equation (4). Following Modugno (2013), we estimate the model with the expectation-maximization (EM) algorithm as detailed in Bańbura and Modugno (2014).

Density construction: Standard bootstrapping procedure

Our procedure closely follows the factor model bootstrapping procedure detailed in Aastveit et al. (2014).

Let T be the number of observations (i.e., the length of the estimation window).

1. Estimate the model specified in equations (2) and (3) to obtain parameter estimates $\hat{A}^{(0)}$, $\hat{B}^{(0)}$, $\hat{C}^{(0)}$, $\hat{Q}^{(0)}$, $\hat{\Sigma}^{(0)}$, $\hat{f}^{(0)}$. Let $\hat{A} = \hat{A}^{(0)}$, $\hat{B} = \hat{B}^{(0)}$, $\hat{C} = \hat{C}^{(0)}$, $\hat{Q} = \hat{Q}^{(0)}$, and $\hat{\Sigma} = \hat{\Sigma}^{(0)}$.
2. For d=1,….,D, do the following
   a. Simulate draws u_t^* from the empirical distribution of $u_t \sim N(0, \hat{Q})$
   b. Generate bootstrap series f_t^* using $\hat{B}\, f_t^* = \hat{A}(L)\, f_{t-1}^* + u_t^*$ where u_t^* is obtained in the previous step
   c. Simulate draws ε_t^* from the empirical distribution of $\varepsilon_t \sim N(0, \hat{\Sigma})$
   d. Generate bootstrap series y_t^* using $y_t^* = \hat{C}\, f_t^* + \varepsilon_t^*$ where ε_t^* and f_t^* are obtained in the previous two steps.
   e. Using y_t^* re-estimate the model in equations (2) and (3) to obtain an updated set of parameter and factor estimates, $\hat{B}^{(d)}$, $\hat{C}^{(d)}$, $\hat{Q}^{(d)}$, $\hat{\Sigma}^{(d)}$, $\hat{f}^{(d)}$. Set $\hat{A} = \hat{A}^{(d)}$, $\hat{B} = \hat{B}^{(d)}$, $\hat{C} = \hat{C}^{(d)}$, $\hat{Q} = \hat{Q}^{(d)}$, and $\hat{\Sigma} = \hat{\Sigma}^{(d)}$
   f. Based on the parameter and factor estimates obtained in the previous step construct forecasts of factors via equation (3), which are then aggregated up to produce nowcasts (and forecasts) for monthly inflation, ${\pi_{t+h}^*}^{(d)}$ via equation (2).
   g. REPEAT
3. The empirical distribution $\{\pi_{t+h}^*\}_{d=1}^{D}$ constitutes the estimate of the density nowcast corresponding to the forecast horizon, h

A.1.3. DMS Model

As discussed in the body of the paper, the DMS model is essentially a collection of univariate and multivariate regressions applied to disaggregate components and aggregate inflation. To appropriately account for uncertainty, we devise two separate bootstrapping algorithms for univariate and multivariate formulations. The difference between these two algorithms is only slight but it helps improve the density accuracy of monthly inflation.

We first describe the general-purpose bootstrap algorithm for the multivariate regression followed by the description for the univariate regression.

A general representation for a multivariate regression can be written as follows,

$$y_t = \beta_0 + \alpha X_t + \varepsilon_t \qquad \varepsilon_t \sim N(0, \sigma^2) \tag{6}$$

Assume that $\hat{\beta}_0, \hat{\alpha}, \hat{\sigma}^2$ are the OLS estimates obtained through the estimation of equation (6) over the sample 1,…,*T*. $\hat{\varepsilon}_t$ are the least squares residuals with mean 0 and variance $\hat{\sigma}^2$.

<u>Density construction, algorithm 1: Wild block bootstrap for density forecasts</u>

For d=1,….,D do the following.

1. Construct a transformed series of residuals $\{\ddot{\varepsilon}_t\}_{t=1}^T$ from the OLS residuals $\{\hat{\varepsilon}_t\}_{t=1}^T$, where $\ddot{\varepsilon}_t = h(\hat{\varepsilon}_t)u_t$ and $u_t \sim N(0,1)$. h is a transformation function that modifies the original least squares residuals to correct them for possible heteroscedasticity. Various choices for h have been suggested in the literature. Following Chernick and LaBudde (2011, Ch. 6, Section 6.6), we set

   $$h(\hat{\varepsilon}_t) = \frac{\hat{\varepsilon}_t}{1-H} \quad \text{where } H = X(X'X)^{-1}X'$$

   We also tried $h(\hat{\varepsilon}_t) = \frac{\hat{\varepsilon}_t}{(1-H)^{1/2}}$, another widely used transformation.

2. Sampling from $\ddot{\varepsilon}$:
   a. To correct for possible serial correlation (following Aastveit et al., 2014), we draw blocks of consecutive errors from $\ddot{\varepsilon}$. We define the block size, $b_{size} = 4$; it is common to set it greater than or equal to the forecast horizon; *T* is the number of observations; and $b_{number} = ceil(\frac{T}{b_{size}})$, is an integer that denotes the number of non-overlapping blocks of consecutive errors.
   b. For *l*=1,…,b_{size} and *j*=1,…,b_{number} construct the bootstrap sample for y^*

      $$y^*_{(j-1)b_{size}+l} = \hat{\beta}_0 + \hat{\alpha}X_{(j-1)b_{size}+l} + \varepsilon^*_{(j-1)b_{size}+l}$$

      where $\varepsilon^*_{(j-1)b_{size}+l} = \ddot{\varepsilon}_{(j-1)b_{size}+l} \cdot \delta_j$, and δ_j is set as a Rademacher variable, following Davidson and Flachaire (2008) and Aastveit et al (2014):

      $$\delta_j = \begin{cases} +1, & with\ probability\ 0.5 \\ -1, & with\ probability\ 0.5 \end{cases}$$

We also experimented with $\delta_j \sim N(0,1)$, but doing so slightly worsened the accuracy of the density forecasts.

3. Based on the bootstrap sample y^*(constructed in the previous step), re-estimate the model in equation (6) to obtain updated estimates $\hat{\beta}_0^{(d)}, \hat{\alpha}^{(d)}, \hat{\sigma}^{2(d)}$.
4. Use $\hat{\beta}_0^{(d)}$ and $\hat{\alpha}^{(d)}$ in equation (6) to generate iterative forecasts, $\hat{y}_{t+h}^{(d)}$ up to h periods ahead. (We also experimented with a modified step 4: when generating iterative forecasts $\hat{y}_{t+h}^{(d)}$ we drew from $\varepsilon^* \sim N(0, var(\varepsilon^*))$ for each h. This alternative made no difference to the overall results.)
5. REPEAT
6. The empirical distribution of $\{\hat{y}_{t+h}\}_{d=1}^{D}$ constitutes our estimate of the *h*-step-ahead density.

Next, we describe the algorithm that we apply to the univariate AR regressions. A general representation for a univariate AR regression is:

$$y_t = \beta_0 + \sum_{j=1}^{P} \alpha_j \, y_{t-j} + \varepsilon_t \qquad \varepsilon_t \sim N(0, \sigma^2) \tag{7}$$

Assume that $\hat{\beta}_0$, $\left[\hat{\alpha}_j\right]_{j=1}^{P}, \hat{\sigma}^2$ are the OLS estimates obtained through the estimation of equation (7) over the sample consisting of 1,…,*T* observations. $\hat{\varepsilon}_t$ are the least squares residuals with mean 0 and variance $\hat{\sigma}^2$.

<u>Density construction, algorithm 2: Parametric bootstrap for density forecasts</u>

For d=1,….,D do the following.

1. Construct a transformed series of residuals $\{\ddot{\varepsilon}_t\}_{t=1}^{T}$ from the residuals $\{\hat{\varepsilon}_t\}_{t=1}^{T}$, where $\ddot{\varepsilon}_t = \left(\frac{T}{T-k}\right)^{0.5} \hat{\varepsilon}_t$ and k is the number of regressors, in this case $k = P + 1$; P is the number of lags of the dependent variable. We also experimented with $\ddot{\varepsilon}_t = h(\hat{\varepsilon}_t)u_t$ and $u_t \sim N(0,1)$ but this produced inferior nowcasts.
2. Sample a sequence of $\{\varepsilon^*\}_{t=1}^{T}$ from $\ddot{\varepsilon} \sim N(0, var(\ddot{\varepsilon}))$ and then construct a bootstrap sample of $\{y^*\}_{t=1}^{T}$ using

$$y_t^* = \hat{\beta}_0 + \sum_{j=1}^{P} \hat{\alpha}_j \, y_{t-j}^* + \varepsilon_t^*$$

3. Based on the bootstrap sample y^* re-estimate the model in equation (7) to obtain updated estimates $\hat{\beta}_0{}^{(d)}, \left[\hat{\alpha}_j{}^{(d)}\right]_{j=1}^{P}$
4. Use $\hat{\beta}_0{}^{(d)}, \left[\hat{\alpha}_j{}^{(d)}\right]_{j=1}^{P}$ in equation (7) to iteratively generate forecasts, $\hat{y}_{t+h}^{(d)}$ up to h periods ahead. (We also experimented with a modified step 4: when generating iterative forecasts $\hat{y}_{t+h}^{(d)}$ we draw from $\ddot{\varepsilon} \sim N(0, var(\ddot{\varepsilon}))$ for each h. This alternative made no difference to the overall results.)
5. REPEAT
6. The empirical distribution of $\{\hat{y}_{t+h}\}_{d=1}^{D}$ constitutes our estimate of the h-step-ahead density.

Using the same notation as in KZ, the general representation of the DMS model for monthly headline (or core) inflation is

$$A_{s(t)}\,\boldsymbol{Z_t} = B_{s(t)} + C_{s(t)}\boldsymbol{X_t} + \sum_{j=1}^{J} D_{j,s(t)}\boldsymbol{Z_{t-j}} + \varepsilon_{s(t)} \tag{8}$$

where $\mathbf{Z}_t$ is an $n \times 1$ vector of aggregates, $\mathbf{X}_t$ is an $m \times 1$ vector of disaggregates that are informative over $\mathbf{Z}_t$, and $\boldsymbol{\varepsilon}_{s(t)} \sim N(\mathbf{0}, \boldsymbol{\Sigma})$. The coefficient matrices **A**, **B**, **C**, and $\mathbf{D}_j$ are $n \times n$, $n \times 1$, $n \times m$, and $n \times n$, respectively, and are allowed to vary over time depending on the available information set, denoted $s(t)$; in particular, **C** and $\mathbf{D}_j$ measure the weights put on the disaggregates and lagged aggregates, respectively.

<u>Nowcasting core inflation</u>

Let $\mathbf{Z}_t = [\pi_t^{\text{Core CPI}}, \pi_t^{\text{Core PCE}}]'$ and $\mathbf{X}_t = \mathbf{0}$ in equation (8). We specify two possible regression specifications for core inflation. The first one is a univariate AR, and the second is a bridge equation (i.e., multivariate regression), which regresses core CPI on core PCE and a constant. Conditional on the available information, equation (8) reduces to either a univariate AR or a combination of a univariate AR and bridge equation.

Univariate AR: $\pi_t^{Core} = \beta_0 + \sum_{j=1}^{P} \alpha_j\, \pi_{t-j}^{Core} + \varepsilon_t$.

Bridge equation: $\pi_t^{CorePCE} = \gamma_0 + \theta\, \pi_t^{CoreCPI} + u_t$.

In cases where we have an additional monthly release of core CPI compared with core PCE, and only core PCE remains to be nowcasted: (1) The forecasts of core CPI are produced using a univariate AR, and algorithm 2 is used to produce density forecasts. (2) The nowcast of core PCE is produced using a bridge regression. The forecasts up to *h* steps ahead are produced using a univariate regression that treats the nowcast from a bridge regression as an initial value. To produce density estimates (nowcasts and forecasts), algorithm 2 is used. In all other cases, both core CPI and core PCE are nowcasted (and forecasted) using a univariate AR model. The density estimates are computed based on algorithm 2.

<u>Nowcasting food inflation</u>

Nowcasts for food inflation are produced and used to nowcast headline inflation in all cases except: (1) when we are unable to produce a nowcast for gasoline inflation, and (2) when we have an additional reading for PCE inflation (π^{PCE}) compared to CPI inflation (π^{CPI}). Similar to core PCE, we adopt a parsimonious approach to produce nowcasts of food inflation by simply estimating a univariate AR,

$$\pi_t^{food} = \beta_0 + \sum_{j=1}^{P} \alpha_j \, \pi_{t-j}^{food} + \varepsilon_t$$

Density nowcasts (and forecasts) are produced using algorithm 2.

<u>Nowcasting gasoline inflation</u>

Following KZ, we generate nowcasts (and forecasts) for gasoline inflation based on the availability of weekly gasoline prices and daily oil prices. If weekly gasoline prices are available in the current month, these form the basis for that month's gasoline inflation nowcast. We use a daily random walk in oil prices to extend (i.e., forecast) the oil price series by one additional month. If oil price data or a forecast for oil prices is available for a month but gasoline prices are not available from within that month, then we produce nowcasts or forecasts for gasoline inflation ($\hat{\pi}^{gasoline}$) via a two-stage regression procedure (see KZ for details). In the first stage, a longer-run relationship between monthly gasoline prices and monthly oil prices is assumed via the following regression:

$$P_{t-1}^{\text{Gasoline (NSA)}} = \alpha + \beta P_{t-1}^{\text{Oil}} + e_{1,t-1} \tag{9}$$

Denote $\tilde{P}_{t-1}^{Gasoline(NSA)}$ as the fitted monthly gasoline prices obtained by estimating equation (9). In the second stage, we estimate an error correction model that uses the lagged gap between gasoline prices and their predicted (longer-run) values obtained in the first stage via the following regression:

$$\Delta P_{t-1}^{\text{Gasoline (NSA)}} = b\Delta P_{t-1}^{\text{Oil}} + c\left(P_{t-2}^{\text{Gasoline (NSA)}} - \tilde{P}_{t-2}^{\text{Gasoline (NSA)}}\right) + e_{2,t-1} \qquad (10)$$

Using the estimated coefficients in equations (9) and (10) and iterating forward equations (9) and (10) we generate $\hat{P}_{t-1+h}^{Gasoline(NSA)}$ and $\widehat{\Delta P}_{t-1+h}^{Gasoline(NSA)}$ and in turn estimates of $\hat{\pi}_{t-1+h}^{Gasoline(NSA)}$. The estimates are seasonally adjusted to produce $\hat{\pi}_{t-1+h}^{Gasoline}$. The density forecasts are produced by applying algorithm 1 sequentially to equations (9) and (10). For each simulation *d*, $\hat{\pi}_{t-1+h}^{Gasoline(NSA),d}$ is seasonally adjusted to obtain the corresponding $\hat{\pi}_{t-1+h}^{Gasoline,d}$.

<u>Nowcasting headline inflation</u>

Let $\mathbf{Z}_t = [\pi_t^{\text{CPI}}, \pi_t^{\text{PCE}}]'$ and $\mathbf{X}_t = \left[\pi_t^{\text{Core CPI}}, \pi_t^{\text{Core PCE}}, \pi_t^{\text{Food}}, \pi_t^{\text{Gasoline}}\right]'$. In cases where we have an additional release of π_t^{CPI}, equation (8) reduces to a bridge equation for π_t^{PCE} and a univariate AR for π_t^{CPI}.

Univariate AR: $\pi_t^{CPI} = \beta_0 + \sum_{j=1}^{P} \alpha_j \pi_{t-j}^{CPI} + \varepsilon_t$.

Bridge equation: $\pi_t^{PCE} = \gamma_0 + \theta\, \pi_t^{CPI} + u_t$.

Density estimates are constructed using algorithm 2. In cases where we have nowcasts of $\hat{\pi}_t^{Gasoline}$, equation (8) reduces to a multivariate regression,

$$\pi_t^{CPI} = b_1 + c_{11}\pi_t^{CoreCPI} + c_{13}\pi_t^{Food} + c_{14}\pi_t^{Gasoline} + e_t^{CPI} \qquad (11)$$

$$\pi_t^{PCE} = b_2 + c_{22}\pi_t^{CorePCE} + c_{23}\pi_t^{Food} + c_{24}\pi_t^{Gasoline} + e_t^{PCE} \qquad (12)$$

The density nowcasts (and forecasts) for CPI and PCE inflation are produced by separately applying algorithm 1 to equations (11) and (12). In very few cases, where we lack estimates of $\hat{\pi}_t^{Gasoline}$ and do not have an additional reading for π_t^{CPI}, equation (8) reduces to univariate AR,

$$\pi_t^{CPI} = \beta_1 + \sum_{j=1}^{P} \alpha_j{}^{CPI} \pi_{t-j}^{CPI} + \varepsilon_t{}^{CPI} \qquad (13)$$

$$\pi_t^{PCE} = \beta_2 + \sum_{j=1}^{P} \alpha_j{}^{PCE} \pi_{t-j}^{PCE} + \varepsilon_t{}^{PCE} \qquad (14)$$

The density nowcasts (and forecasts) are generated by separately applying algorithm 2 on equations (13) and (14).

In all of our simulation procedures, *D*=500. Early experimentation suggested that we would normally obtain similar results if we instead set *D*=1000.

A.2. Mechanics of Density Combination and Graphical illustration

Assume at time *t*, we have $i = 1, \dots, M$ (potentially different) empirical distributions $f_{i,t}(y_t)$ for a variable y_t. We wish to combine them using a given set of M weights, $w_{i,t}$.

Step 1: Looking across all the M empirical distributions, $f_{i,t}(y_t)$, determine the (global) minimum value and (global) maximum value of y_t. Denote x_t^{min} as the minimum value and x_t^{max} as the maximum value.

Step 2: Define a grid $x_t \in \{x_t^{min}, \dots, x_t^{max}\}$ of *S* equally spaced intervals such that $x_{k-1} < x_k$.

Step 3: Transform each of the $i = 1, \dots, M$ empirical distributions $f_{i,t}(y_t)$ to a probability density function (pdf), $p_{i,t}(y_t)$ using the grid x_t as the domain. The Gaussian kernel function (Matlab: ksdensity function) is applied to construct a smoothed $p_{i,t}(y_t)$. Using the same grid x_t to construct each of the M pdfs will guarantee that all the pdfs that are to be combined together at time *t* have the same domain; that is, they are all positioned over the same grid.

Step 4: With all pdfs positioned over the same domain (grid), the combination can be achieved by simply adding up the M different densities using the corresponding weights $w_{i,t}$ (for linear combination) or raised to a power of $w_{i,t}$ for a log pool combination. The combined density $g_t(y_t)$ will also be positioned over the same grid (domain) x_t as the M individual densities.

We set *S*=500. Early experimentation suggested that the results were very similar if we set *S*=1000.

Note that our procedure dynamically adjusts the grid x_t at each time *t*. Alternatively, we could just set it to a predefined interval but then the interval has to be wide enough to encompass all the individual empirical distributions for all *t*=1,…,*T* (i.e., over the evaluation sample). Given the breadth of our analysis, including the number of variables considered and both monthly and quarterly rates, having a grid that adjusts dynamically was more efficient for our application.

In implementing our algorithm, we have benefitted from and are grateful for the PROFOR Matlab toolbox (developed by researchers at the Norges Bank, Bank of England, and Warwick Business School). We have modified some of the functions of the toolbox to fit our needs.

A.3. Comparing Properties of Grand Combinations across Weighting Schemes

Figure 8 in the body of the paper shows the weights and higher-order moments from using the log score weighting scheme to generate the stage 1 and stage 2 combinations. Figures A15, A16, and A17 show the weights and higher-order moments from the CMG, Ganics, and CRPS weighting schemes, respectively. We summarize six key results from this comparison.

First, for CPI inflation and PCE inflation, the DMS combination gets the highest weight in all weighting schemes with the exception of Ganics. Furthermore, the DMS maintains its ranking with incoming information over the course of the month.

Second, the CMG and Ganics grand combinations for CPI inflation and PCE inflation provide stronger evidence of both kurtosis and skewness than the combination based on log score weights. This finding is associated with the grand combination being composed of more diverse components in these cases; that is, the DMS combination, the DFM combination, and the MIDAS combination are all assigned nonzero weights in the grand combination. Different weighting schemes can lead to combinations with very different compositions, as is evident by very different profiles of the weights assigned to the three model classes over time. In general, the greater the diversity in the composition of the grand combination, the greater is the evidence of skewness and kurtosis.[1] But greater flexibility in terms of accommodating skewness and kurtosis does not necessarily translate into improved accuracy. We say this because for CPI inflation the grand combination based on the log-score weighting scheme is more accurate than grand combinations based on other schemes, yet it displays less evidence of skewness and kurtosis on average compared with other grand combinations. This improved accuracy is mainly

[1] We highlight a result in regard to grand combinations for CPI inflation (case 4) produced using the log score weighting scheme (see Figure 8) and the CMG weighting scheme (Figure A15). Both schemes assign a weight of 100% to DMS at least in the last few years of the evaluation sample, yet the profiles of the kurtosis property of the grand combinations across the two schemes are very different for this period. This finding arises in part because the underlying composition of the two respective stage 1 DMS combinations is quite different; see Figure A18.

coming from the significantly more accurate mean of the density nowcast constructed from the log-score scheme, which puts high weight on the stage 1 DMS combination, compared with grand combinations based on other weighting schemes.

Third, in the case of core inflation, the patterns observed in the properties of the grand combination are generally comparable across the various weighting schemes, even though the weights assigned to the densities of the three modeling classes differ. This result stems from the fact that the estimates of density nowcasts for core inflation are generally similar across the different modeling classes; so irrespective of the approach used to combine the component density nowcasts, the resulting estimates of the combined density nowcasts are similar. This latter pattern also explains the comparable accuracy results for core inflation shown in Figures 4 and 5 (especially in the case of core CPI). Relatedly, the weight profiles across different weighting schemes (for core inflation) indicate a high incidence of fast switching across the three combinations. The evidence of time-varying switching across density combinations highlights the importance of combining density estimates from a range of models to circumvent the instability issues of using a single model.

Fourth, the CRPS weighting scheme assigns positive weights to the three combinations across all inflation measures and at all representative dates (shown for cases 1 and 4), reflecting the generous assessment of the CRPS metric. In the case of core inflation, the weights are pretty evenly distributed across the DMS, DFM, and MIDAS combinations.

Fifth, in our application, the two optimal combination weighting schemes (CMG and Ganics) yield weight profiles that are remarkably different, especially in the case of CPI inflation and PCE inflation. However, the different profiles are not unexpected, given the earlier results that showed MIDAS and DFM combinations producing well-calibrated densities compared with DMS, which tends to do quite well in relative accuracy scoring. The weights produced from the Ganics approach display quite a bit of variability early in the sample. This variability is also present to a degree in the results reported in Ganics (2017) using industrial production data.

A.4. Additional References

Chernick, Michael R., and Robert A. LaBudde. 2011. *An Introduction to Bootstrap Methods with Applications to R.* John Wiley and Sons.

Davidson, Russell, and Emmanuel Flachaire. 2008. “The Wild Bootstrap, Tamed at Last.” *Journal of Econometrics* 146(1): 162-69. https://doi.org/10.1016/j.jeconom.2008.08.003.

Davidson, Russell, and James G. MacKinnon. 2006. “Bootstrap Methods in Econometrics.” In Kerry Patterson and Terence C. Mills, eds. *Palgrave Handbook of Econometrics: Vol 1, Econometric Theory*.

Figure A1: Illustration of Combining Densities with Linear and Log Opinion Pools

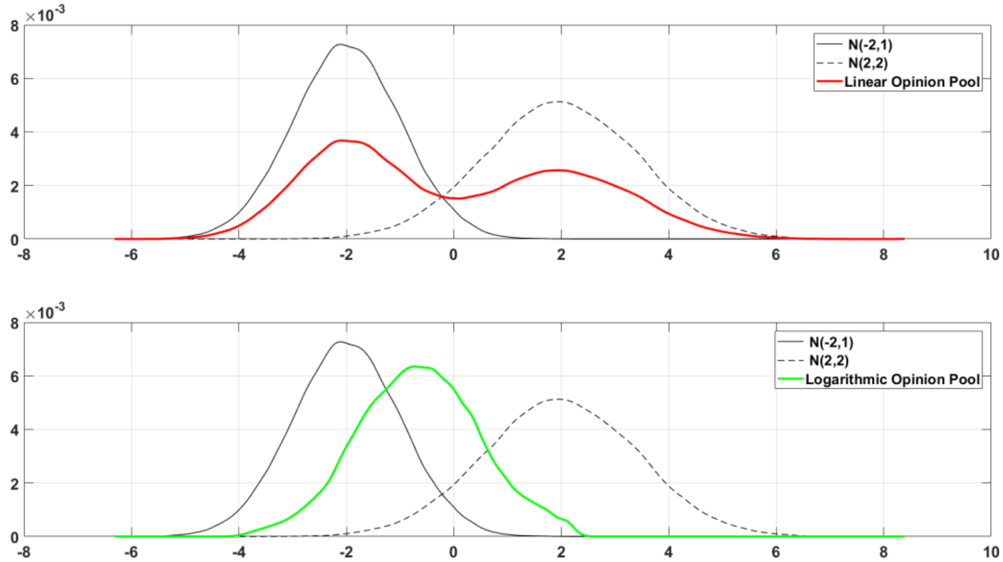

Notes: A simple example (motivated by Kascha and Ravazzolo, 2010) on combining two densities with very different mean and variances via two different functional forms.

Figure A2: Example Stage 1 DMS Combination
Month-over-month inflation (%)

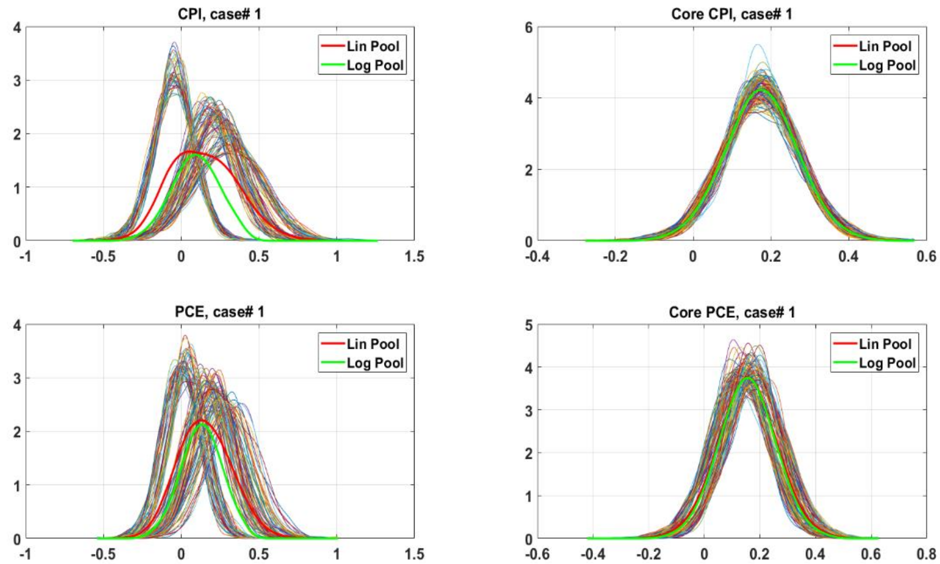

Notes: Single specification density nowcasts (thin lines) underlying the stage 1 DMS combination, linear pool nowcasts (thick red lines), and log pool nowcasts (thick green lines) for case 1 for the month of September 2000.

Figure A3: Comparisons between Single Specifications vs. Stage 1 Combinations

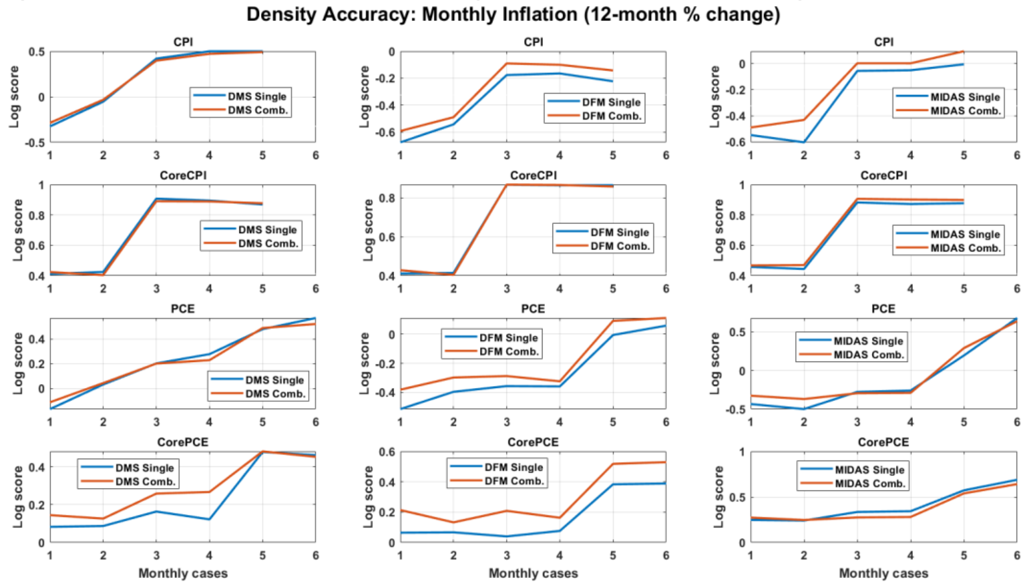

Notes: Average log scores at different nowcast origins for single specifications and stage 1 combinations within model classes. The evaluation sample is September 2000 through June 2015. We exclude September 2001 and October 2001 from the average log score calculations for PCE inflation and core PCE inflation.

Figure A4: Real-Time Density Nowcasts

(a) CPI inflation

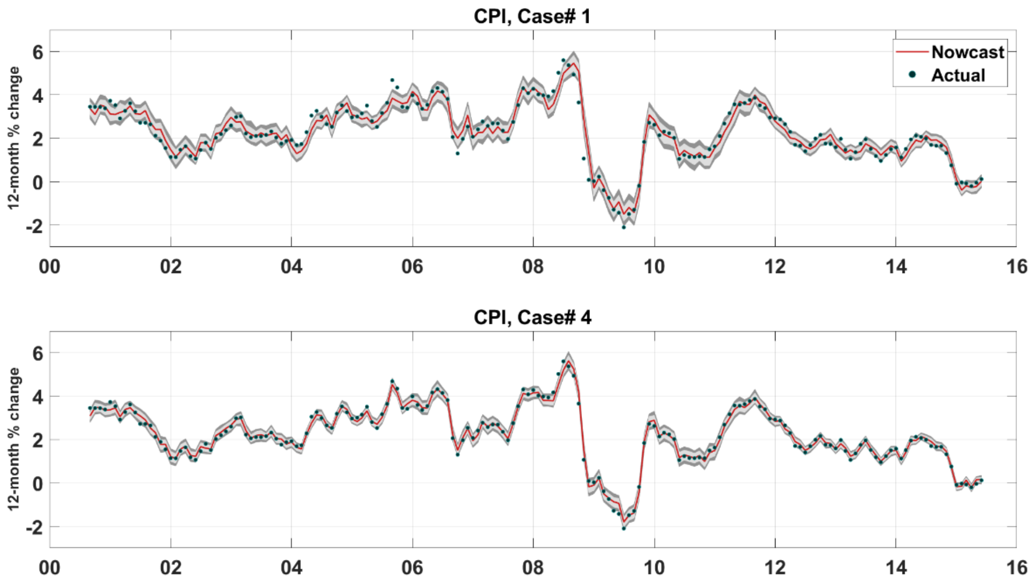

(b) Core CPI inflation

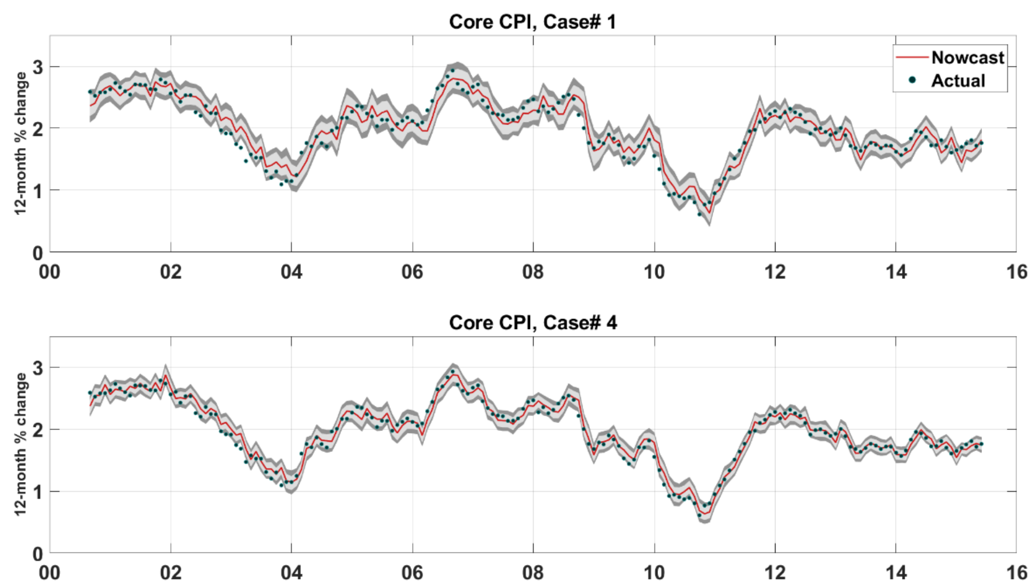

Figure A4: Real-Time Density Nowcasts (continued)

(c) PCE inflation

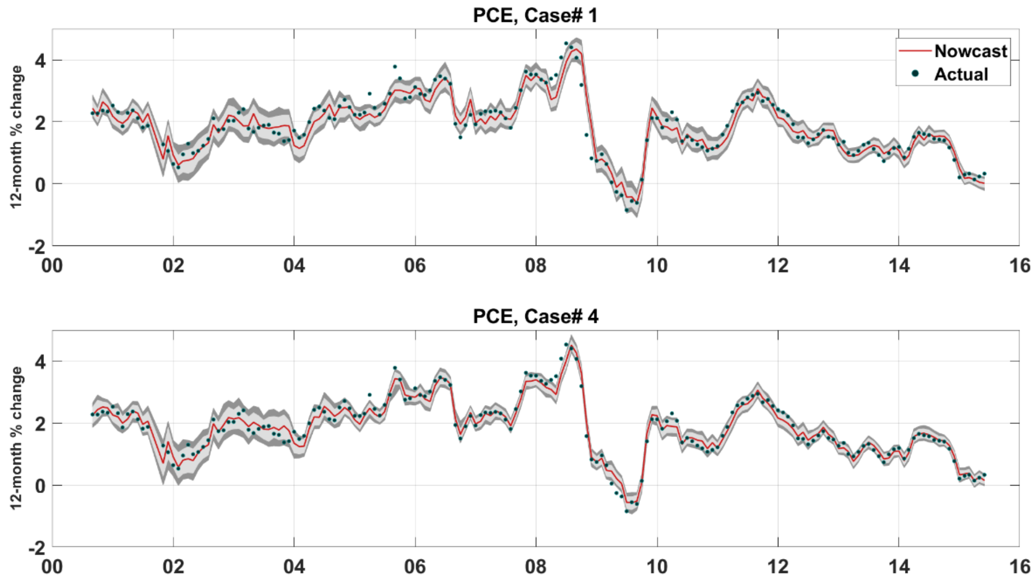

(d) Core PCE inflation

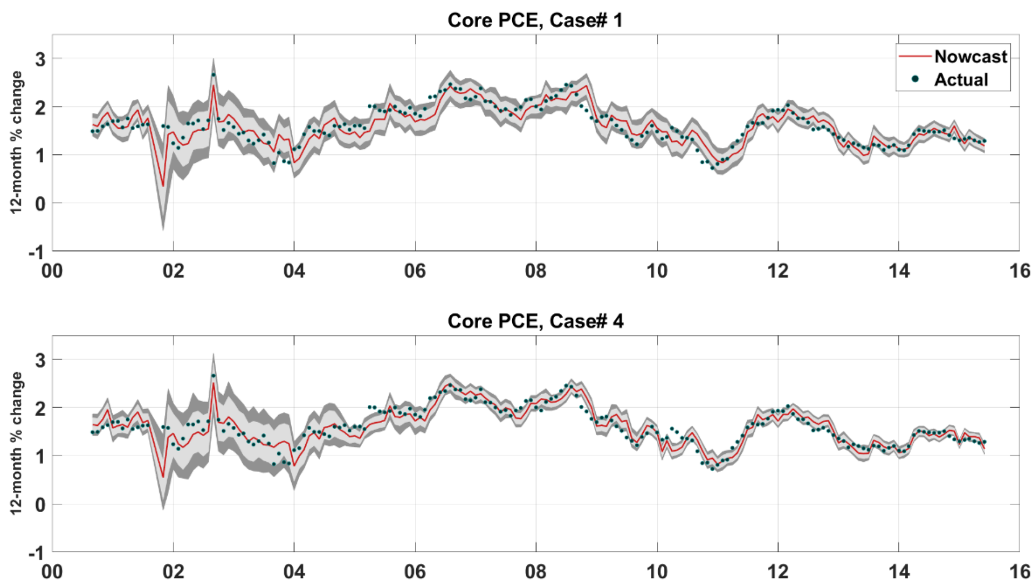

Notes: The figure shows the out-of-sample nowcasts generated using real-time data from the grand combination with the log score weighting scheme and the flexible aggregation strategy at two different points in each month (case 1 and case 4) for the 12-month trailing inflation rate. The shaded areas represent 70% and 90% prediction intervals. The sample period spans September 2000 through June 2015.

Figure A5: Weights Underlying Grand Combination based on Ganics Weighting Scheme

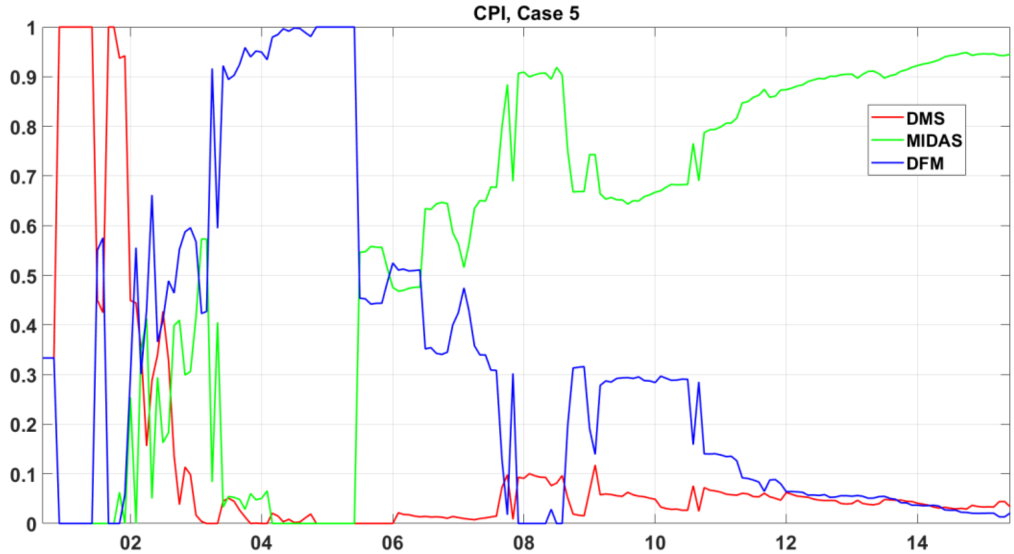

Notes: The figure plots the evolution of the weights applied to each of the stage 1 density combinations from the DMS, MIDAS, and DFM model classes to form the stage 2 combination, based on nowcasts generated for monthly (year-over-year) inflation at case 5 for nowcasting CPI inflation. The sample period spans September 2000 through June 2015.

Figure A6: Density Performance of Grand Combination vs. Its Components: Month-Over-Month Inflation

(a) Relative accuracy based on log score

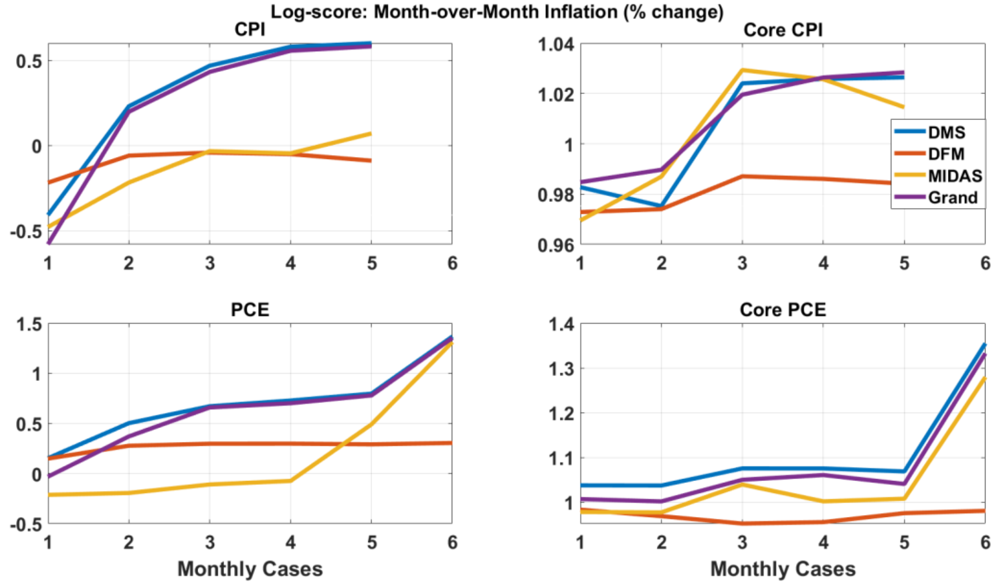

(b) Relative accuracy based on CRPS

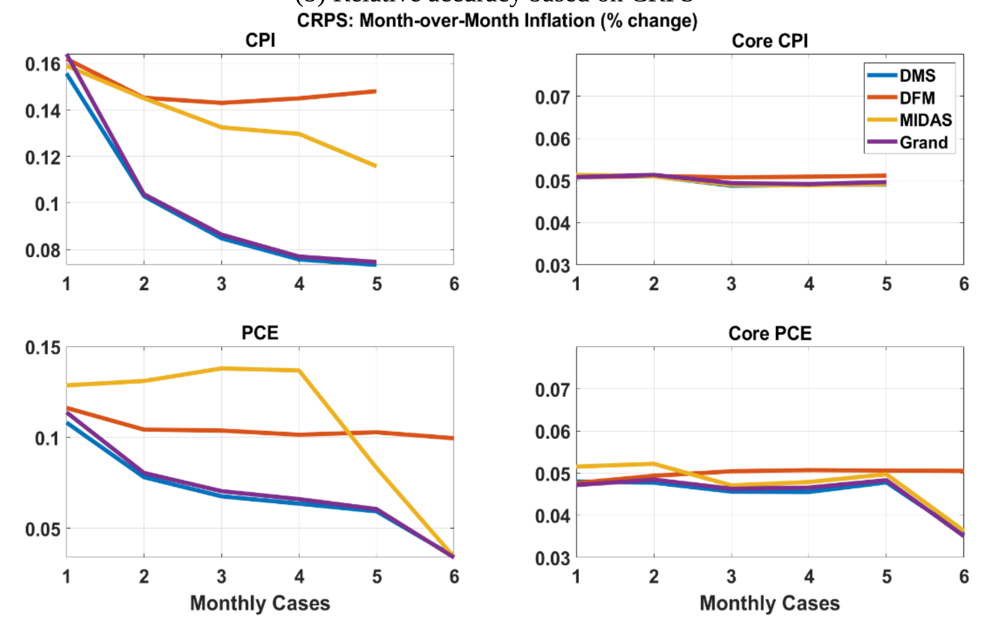

Notes: The top panel plots the average log score and the bottom panel plots the average CRPS for the grand combination based on the log score weighting scheme and combinations based on the DMS model class, MIDAS model class, and DFM model class, where each individual model class uses the log score weighting scheme. The evaluation sample runs from September 2000 through June 2015; we omit September 2001 and October 2001 for PCE inflation and core PCE inflation calculations.

Figure A7: Point Nowcasting Performance, Grand Combination vs. DMS: Month-Over-Month Inflation

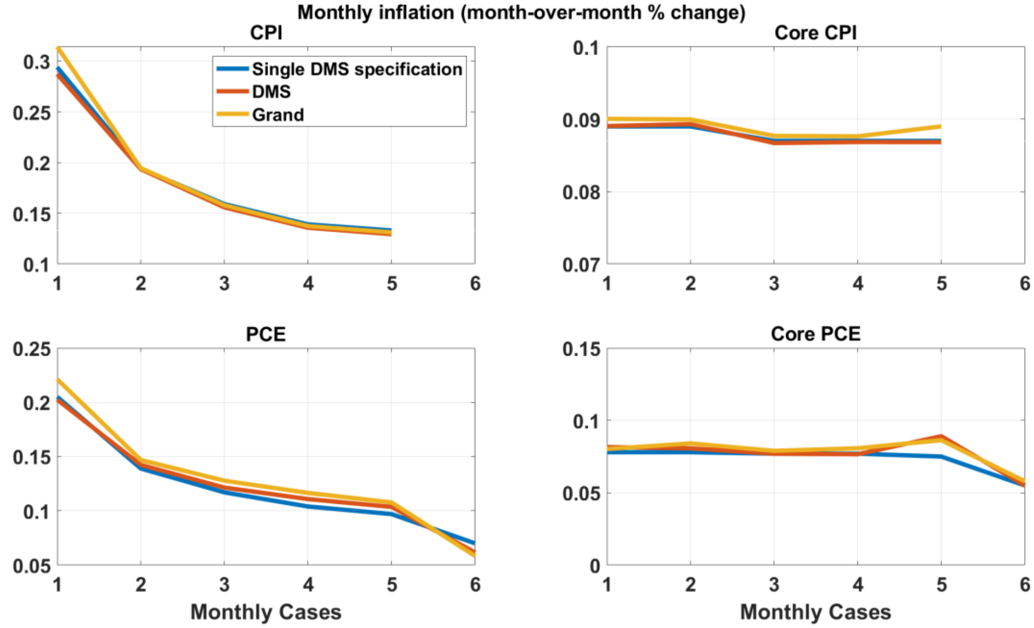

Notes: The figure plots the RMSE for the grand combination based on log score and using the flexible aggregation strategy; the stage 1 combination from the DMS model class; and a single specification from the DMS model class based on Knotek and Zaman (2017). The cases reflect the point in time when each nowcast was made relative to the target nowcast month; see Table 2. The evaluation sample runs from September 2000 through June 2015; we omit September 2001 and October 2001 for PCE inflation and core PCE inflation calculations.

Figure A8: Density Performance of Grand Combination vs. Its Components: Quarterly Inflation

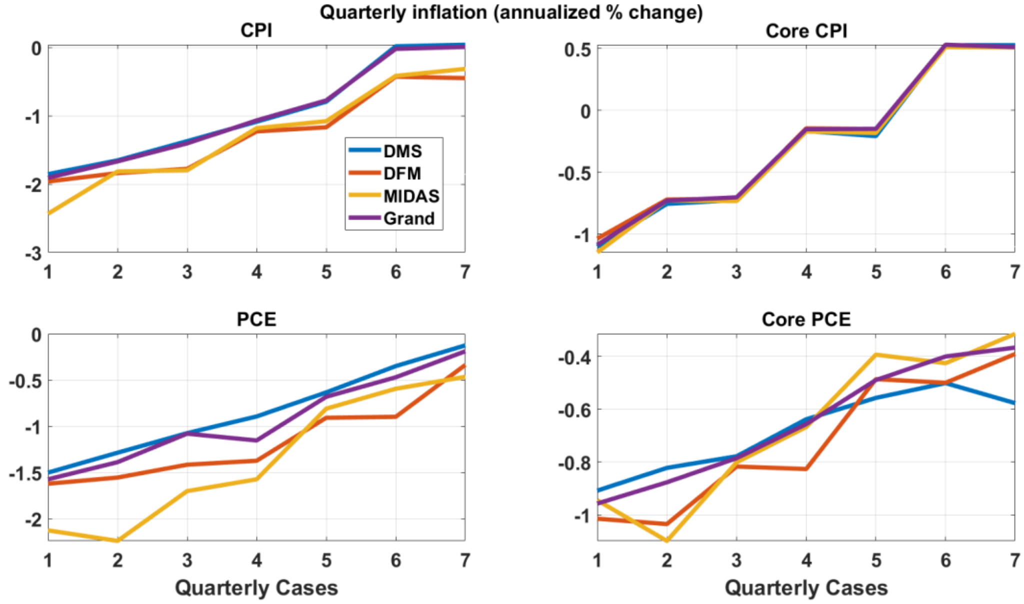

Notes: Average log score for the grand combination based on the log score weighting scheme and combinations based on the DMS model class, MIDAS model class, and DFM model class, where each individual model class uses the log score weighting scheme. The evaluation sample runs from 2000Q4 through 2015Q2; we omit 2001Q3 and 2001Q4 for PCE inflation and core PCE inflation calculations.

Figure A9: Point Nowcasting Performance, Grand Combination vs. Other Combinations and Single DMS Specification: Quarterly Inflation

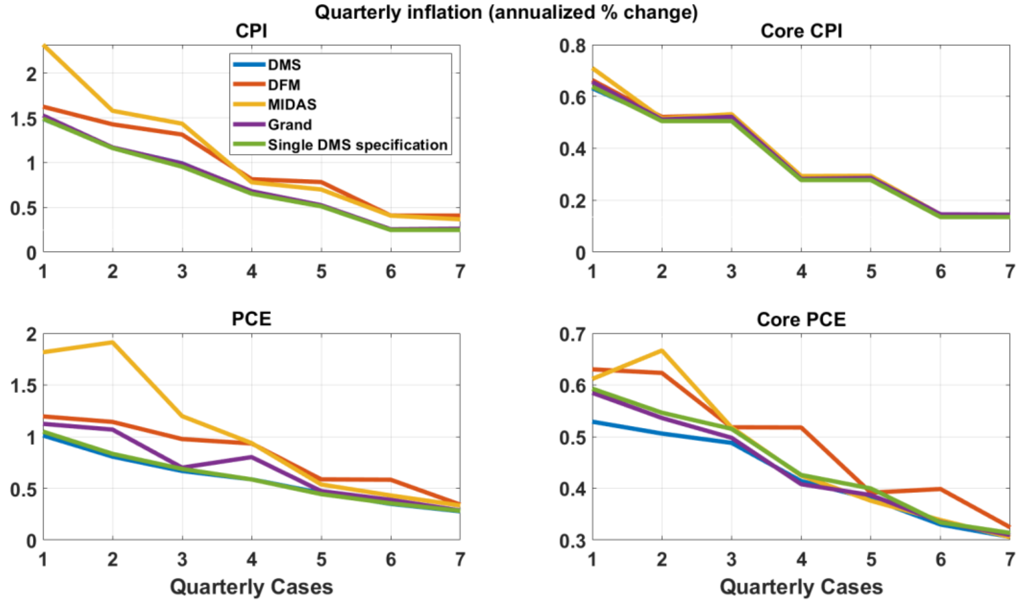

Notes: The figure plots the RMSE for the grand combination based on log score and using the flexible aggregation strategy; the stage 1 combinations from the DMS model class, DFM model class, and MIDAS model class; and a single specification from the DMS model class based on Knotek and Zaman (2017). The cases reflect the point in time when each nowcast was made relative to the target nowcast quarter; see Table 2. The evaluation sample runs from 2000Q4 through 2015Q2; we omit 2001Q3 and 2001Q4 for PCE inflation and core PCE inflation calculations.

Figure A10: Weights for Stage 1 DMS Combinations, Log Score Weighting Scheme

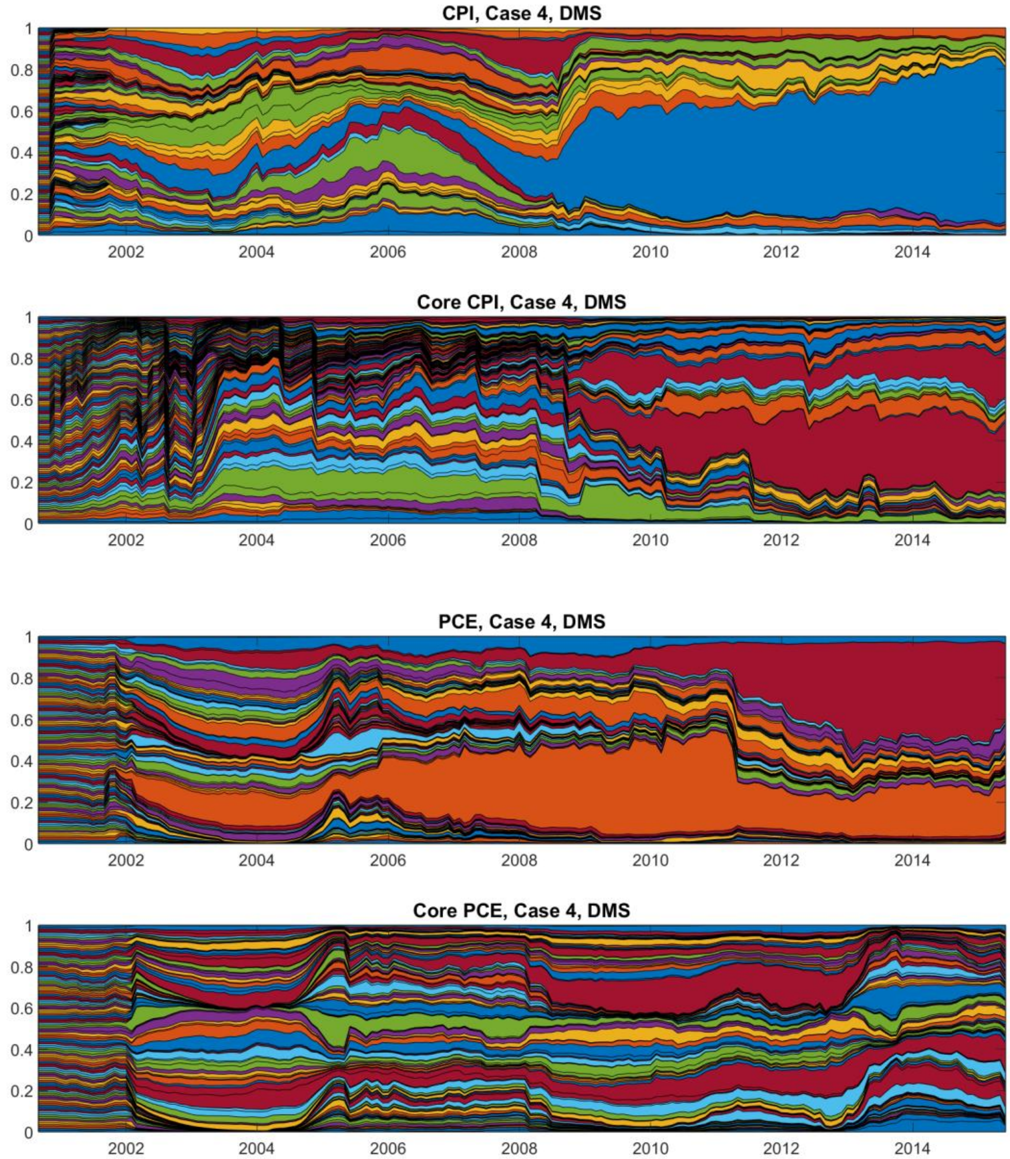

Notes: The figure plots the evolution of the weights for underlying individual candidate densities for the stage 1 DMS combination at case 4. Each color shade represents a particular individual candidate density. There are 108 candidate densities. The sample period spans September 2000 through June 2015.

Figure A11: Weights for Stage 1 DFM Combinations, Log Score Weighting Scheme

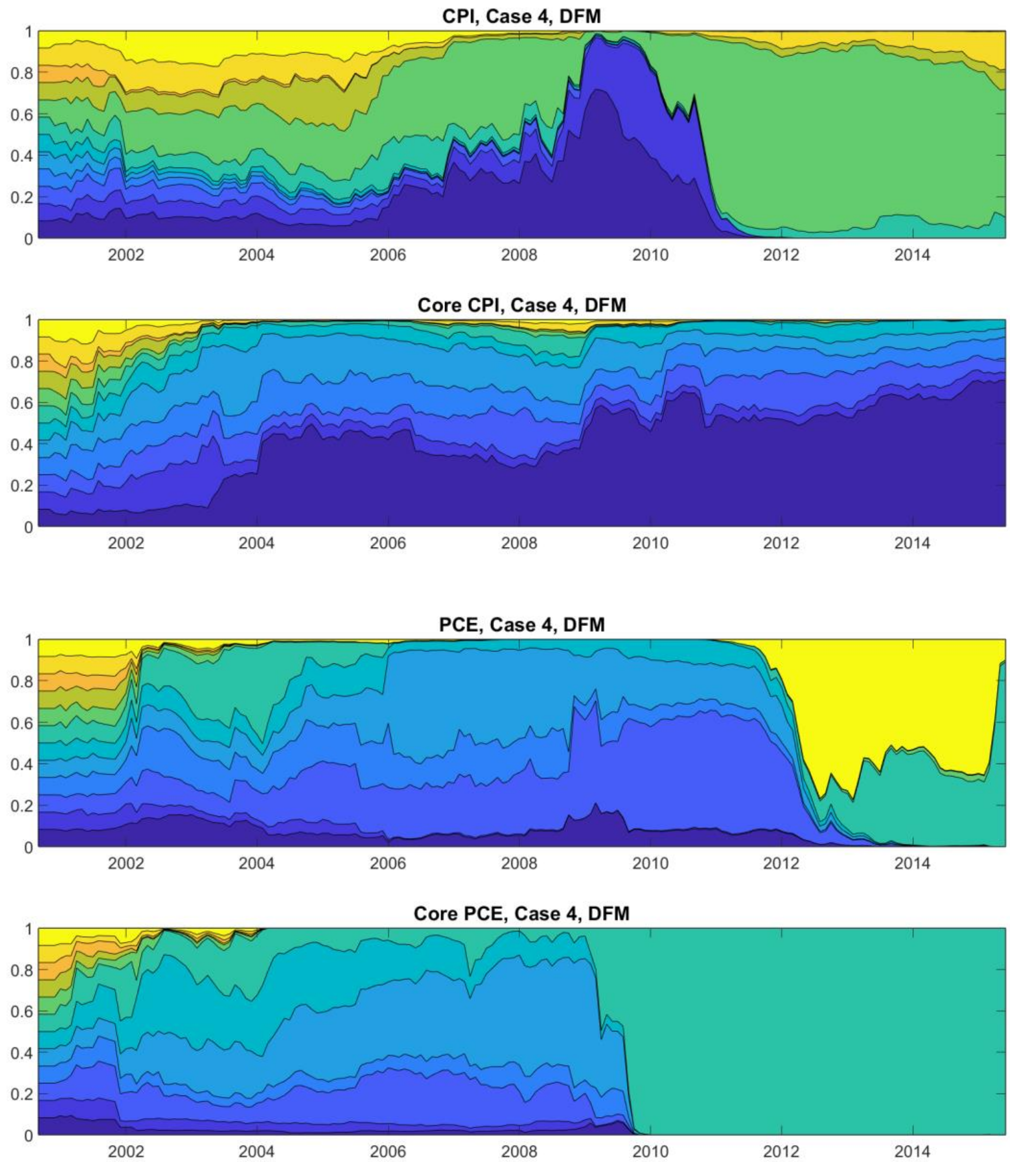

Notes: The figure plots the evolution of the weights for of underlying individual candidate densities for the stage 1 DFM combination at case 4. Each color shade represents a particular individual candidate density. There are 12 candidate densities. The sample period spans September 2000 through June 2015.

Figure A12: Weights for Stage 1 MIDAS Combinations, Log Score Weighting Scheme

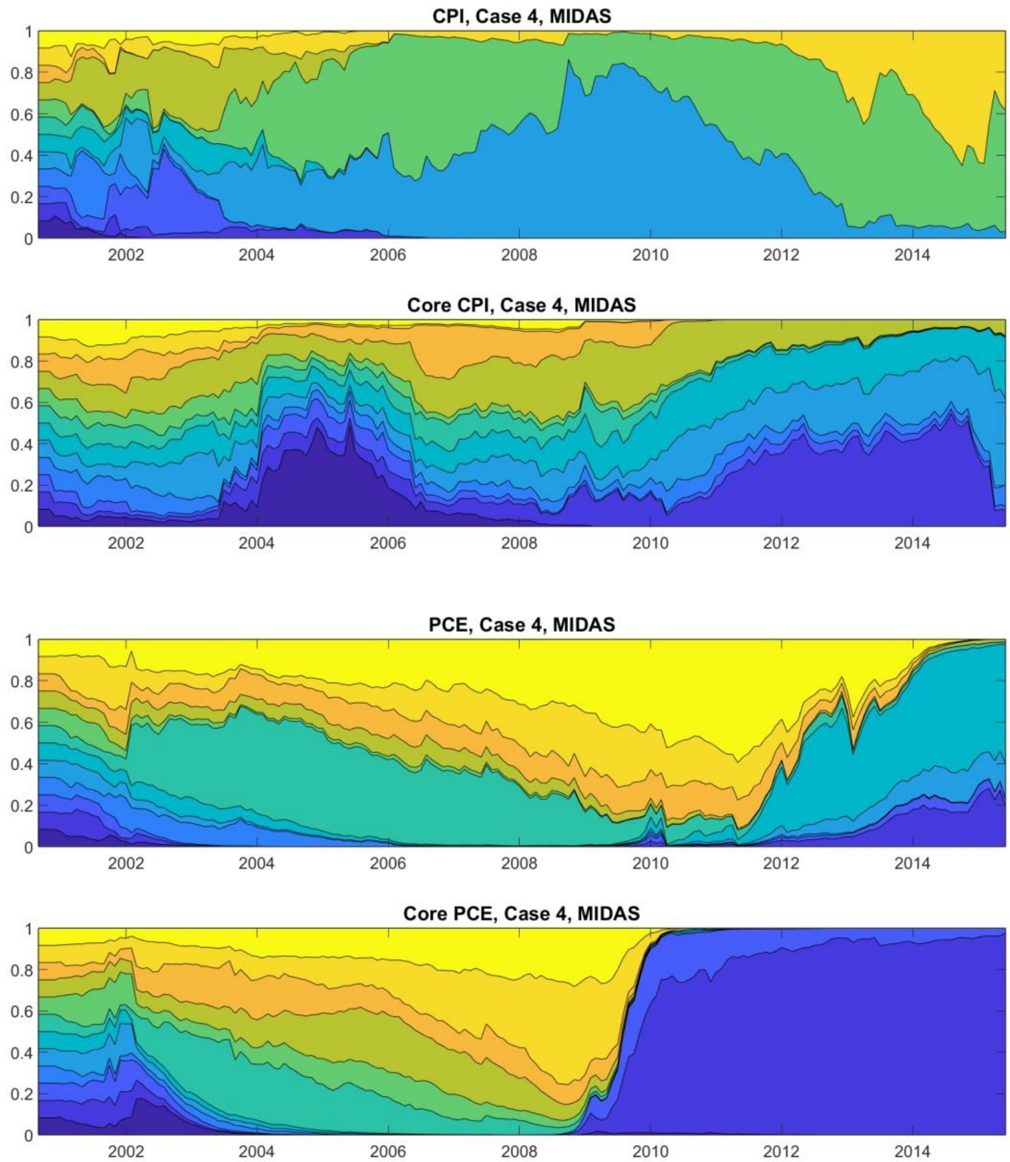

Notes: The figure plots the evolution of the weights for underlying individual candidate densities for the stage 1 MIDAS combination at case 4. Each color shade represents a particular individual candidate density. There are 12 candidate densities. The sample period spans September 2000 through June 2015.

Figure A13: Time-Varying Uncertainty Estimates for Density Nowcasts of Quarterly Inflation

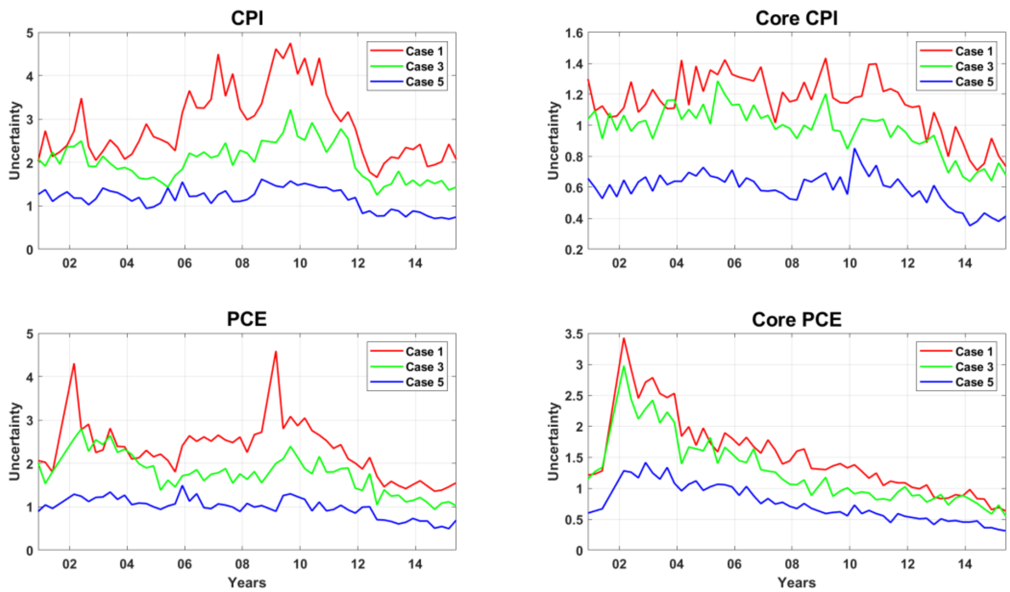

Notes: Uncertainty is measured as the width of the 70% prediction intervals. Estimates are for the grand combination based on the flexible aggregation strategy and log score weighting scheme for case 1 (last day of the preceding quarter), case 3 (last day of the first month of the quarter), and case 5 (last day of the second month of the quarter); see Table A1. The sample period spans 2000Q4 through 2015Q2.

Figure A14: Stage 2 Grand Combination of DMS, DFM, and MIDAS Combinations

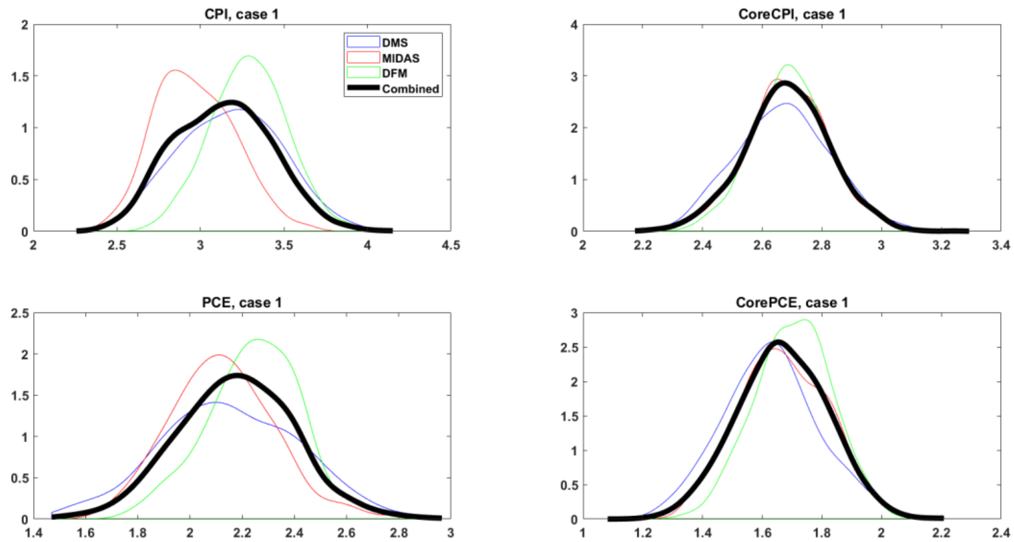

Notes: The figure illustrates a grand combination for 12-month inflation rates as of case 1 (the last day of the previous month) for nowcasting the target month of January 2001 and the three stage 1 combinations from the DMS, MIDAS, and DFM model classes that are used to construct the grand combination.

Figure A15: Weights and Higher-Order Moments, CMG Weighting Scheme

(a) CPI inflation

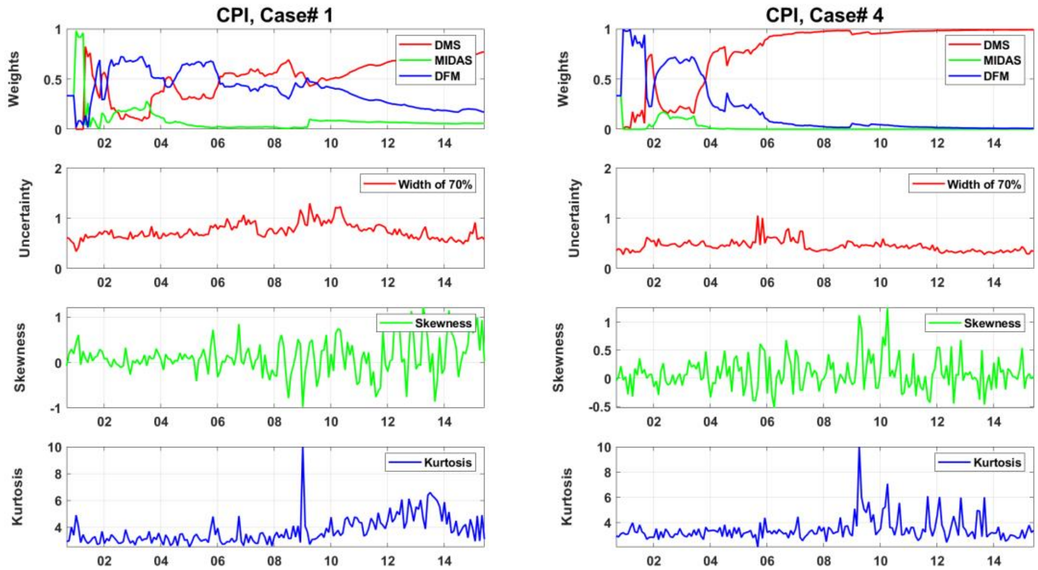

(b) Core CPI inflation

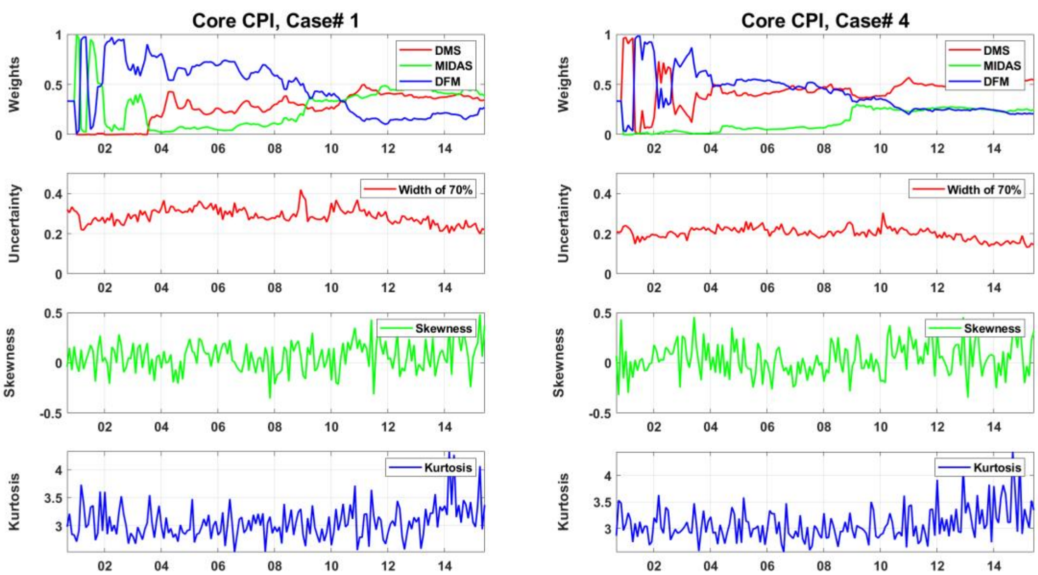

Figure A15: Weights and Higher-Order Moments, CMG Weighting Scheme (continued)

(c) PCE inflation

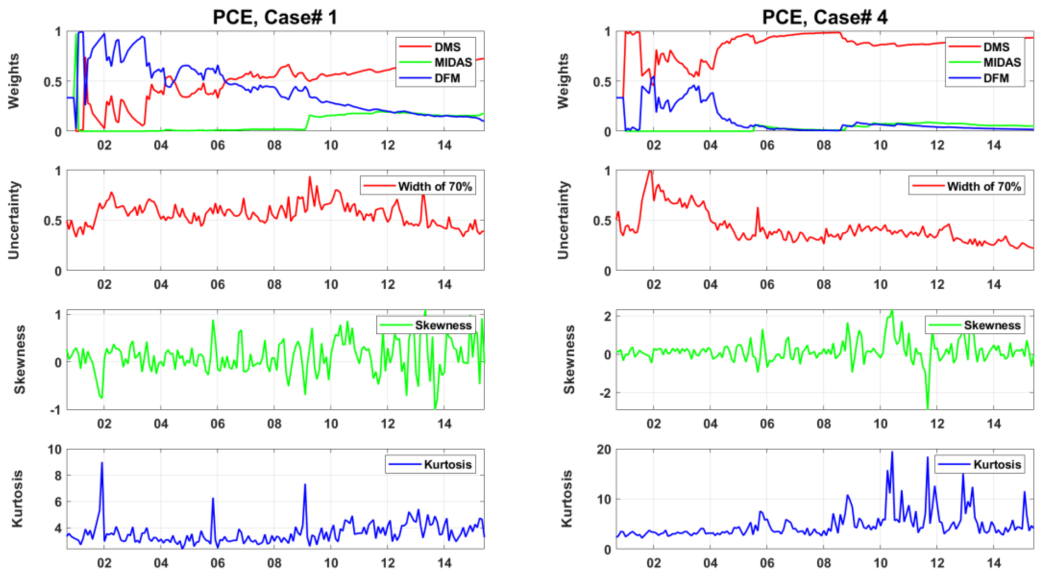

(d) Core PCE inflation

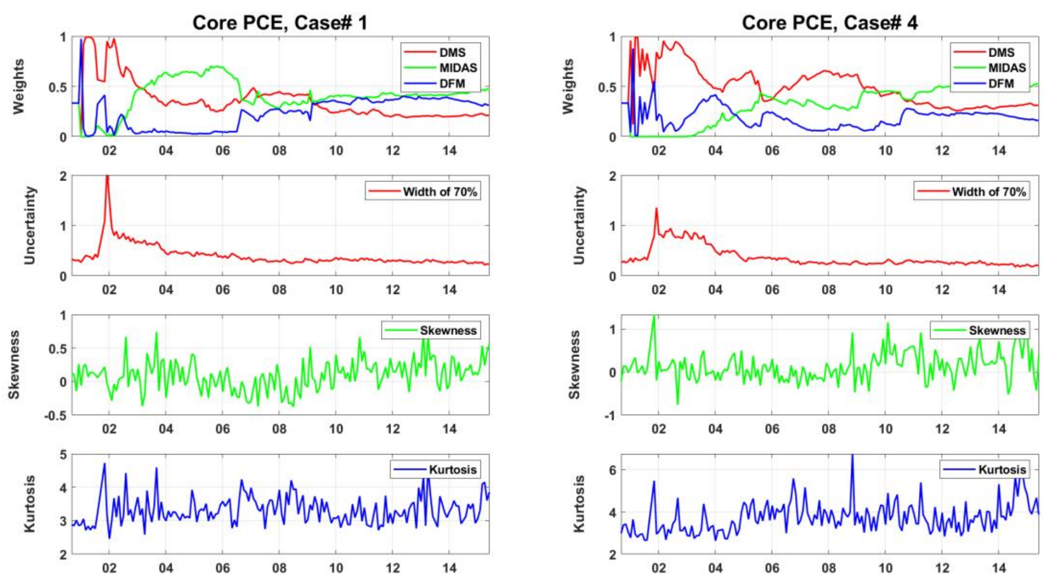

Notes: The first row of each panel plots the evolution of the weights for the three model classes underlying the grand combination, based on the flexible aggregation strategy and CMG weighting scheme. (Each model class is a combination of multiple model specifications.) The second row plots estimates of dynamic uncertainty, defined as the width of the 70% prediction intervals. The last two rows plot time-varying estimates of skewness and kurtosis. The sample period spans September 2000 through June 2015.

Figure A16: Weights and Higher-Order Moments, Ganics Weighting Scheme

(a) CPI inflation

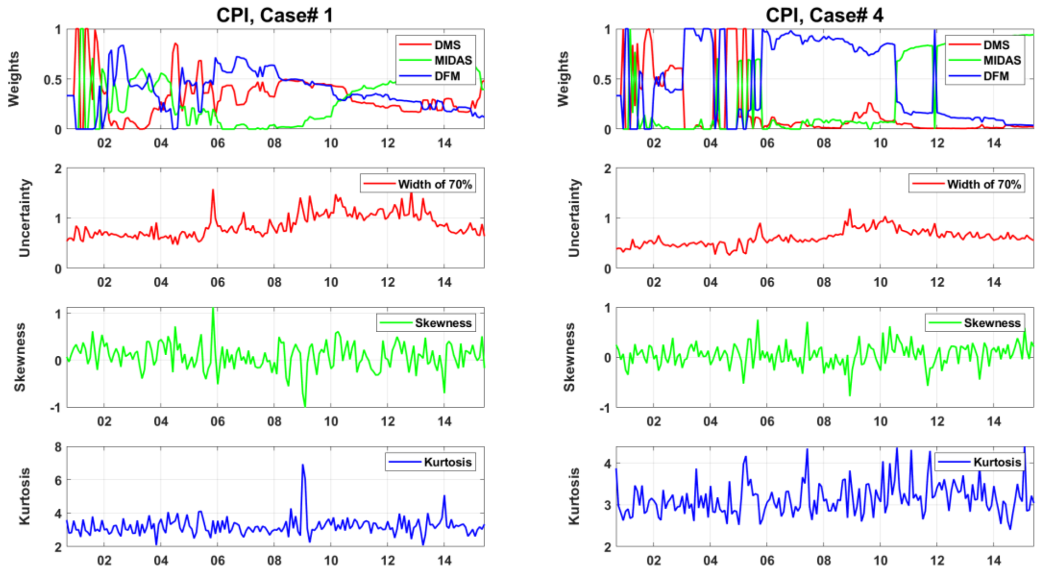

(b) Core CPI inflation

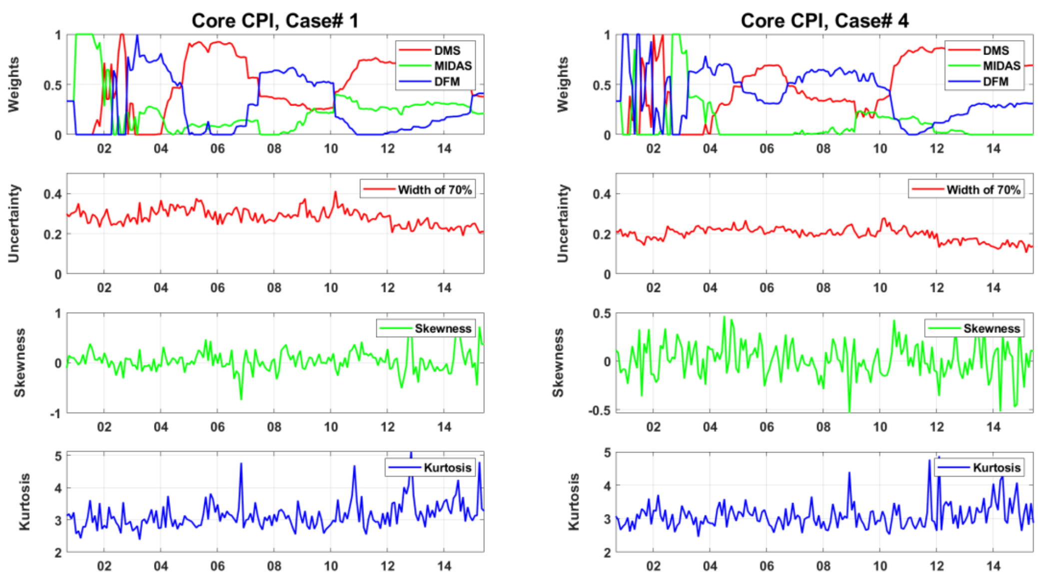

Figure A16: Weights and Higher-Order Moments, Ganics Weighting Scheme (continued)

(c) PCE inflation

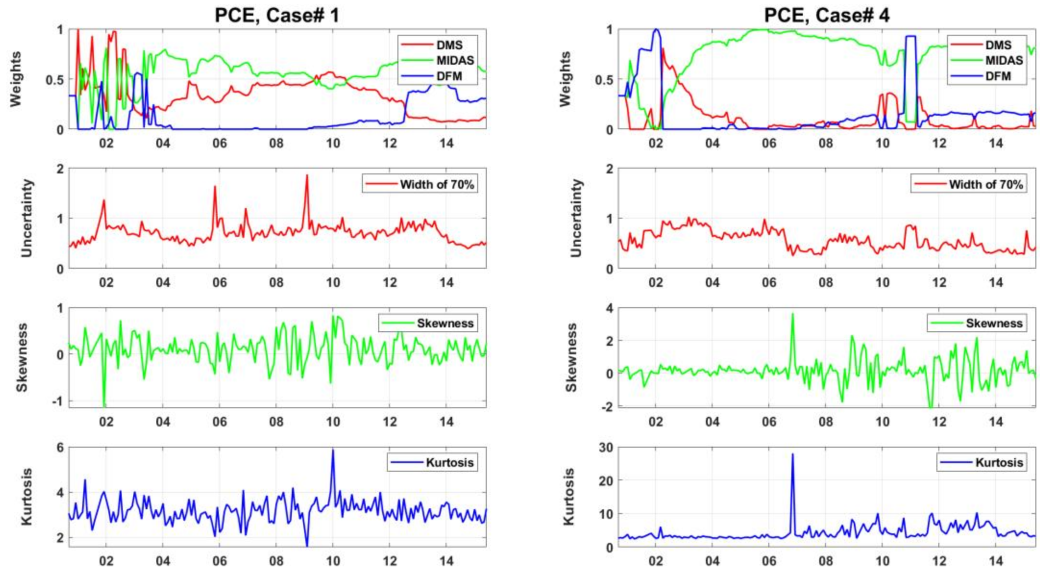

(d) Core PCE inflation

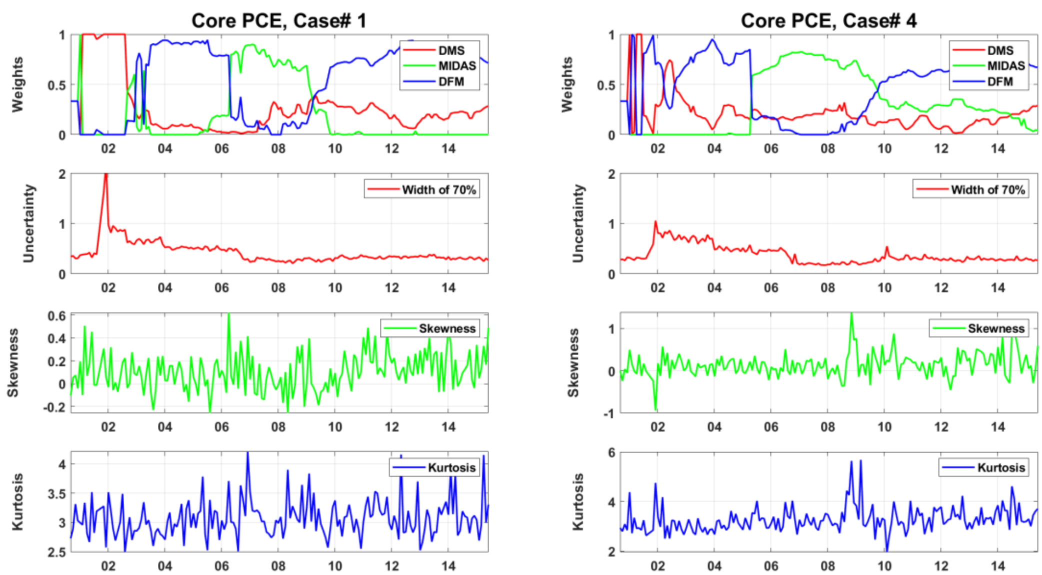

Notes: The first row of each panel plots the evolution of the weights for the three model classes underlying the grand combination, based on the flexible aggregation strategy and the Ganics weighting scheme. (Each model class is a combination of multiple model specifications.) The second row plots estimates of dynamic uncertainty, defined as the width of the 70% prediction intervals. The last two rows plot time-varying estimates of skewness and kurtosis. The sample period spans September 2000 through June 2015.

Figure A17: Weights and Higher-Order Moments, CRPS Weighting Scheme

(a) CPI inflation

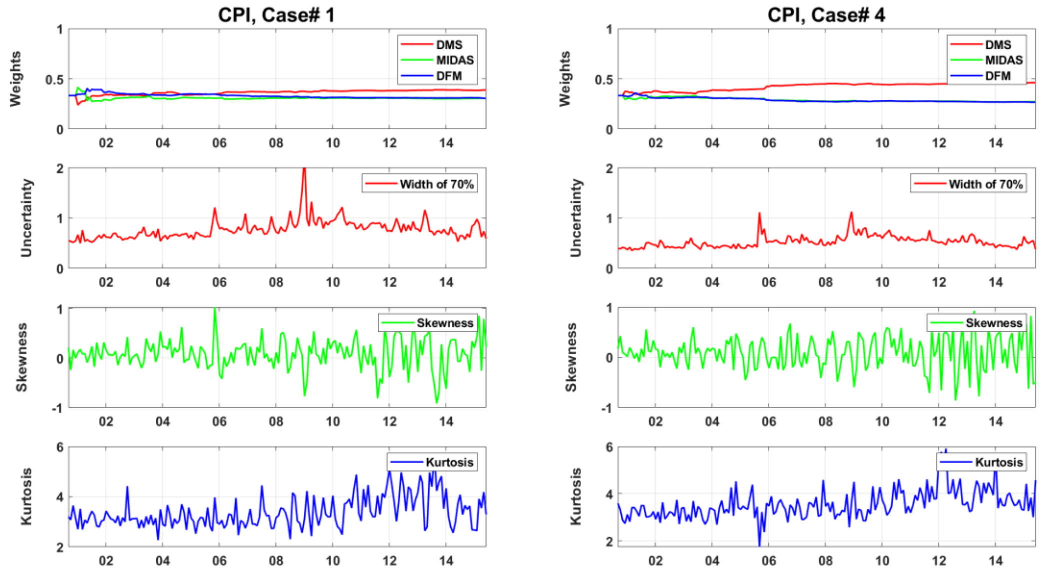

(b) Core CPI inflation

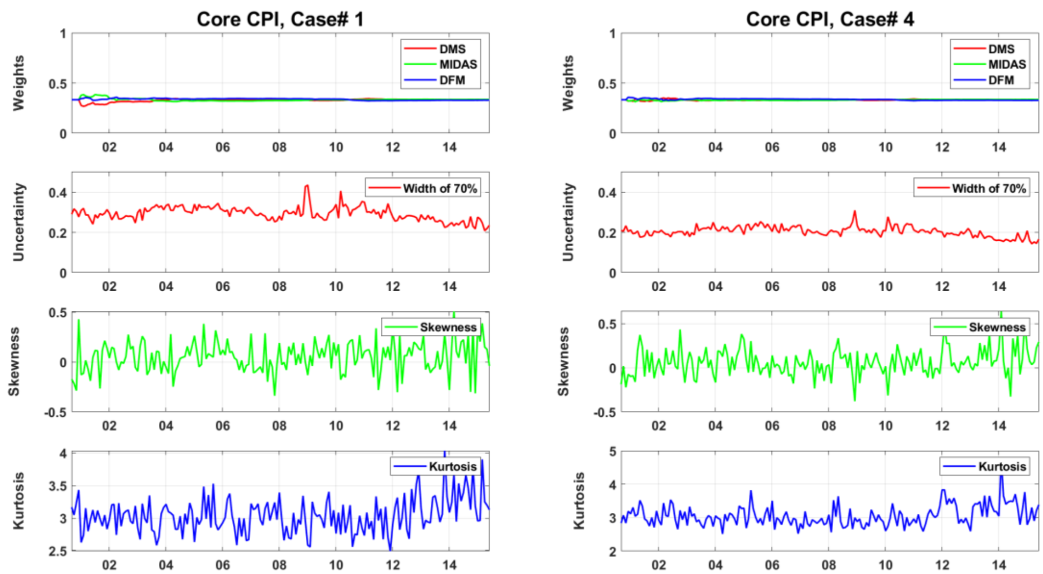

Figure A17: Weights and Higher-Order Moments, CRPS Weighting Scheme (continued)

(c) PCE inflation

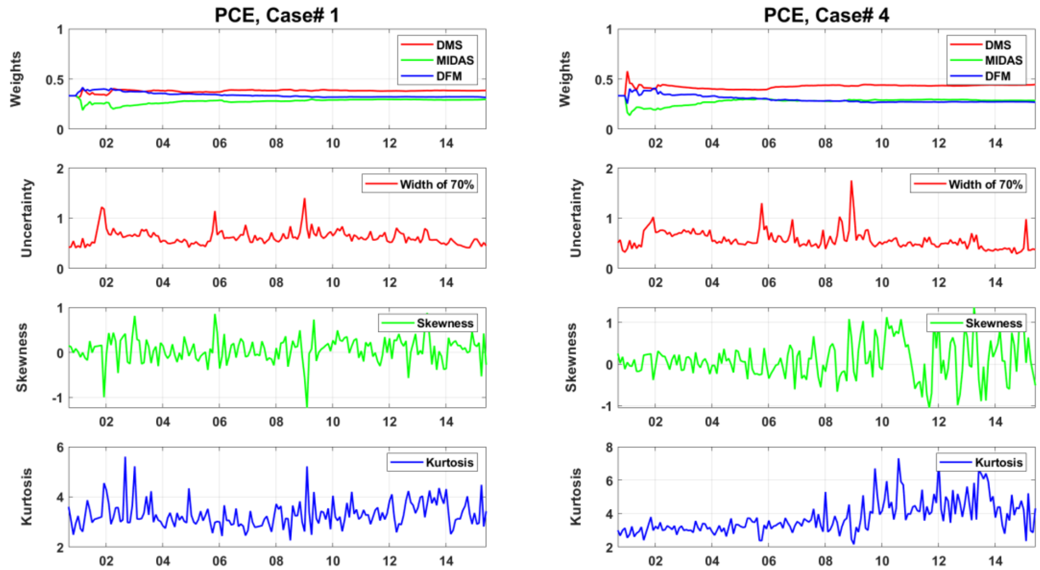

(d) Core PCE inflation

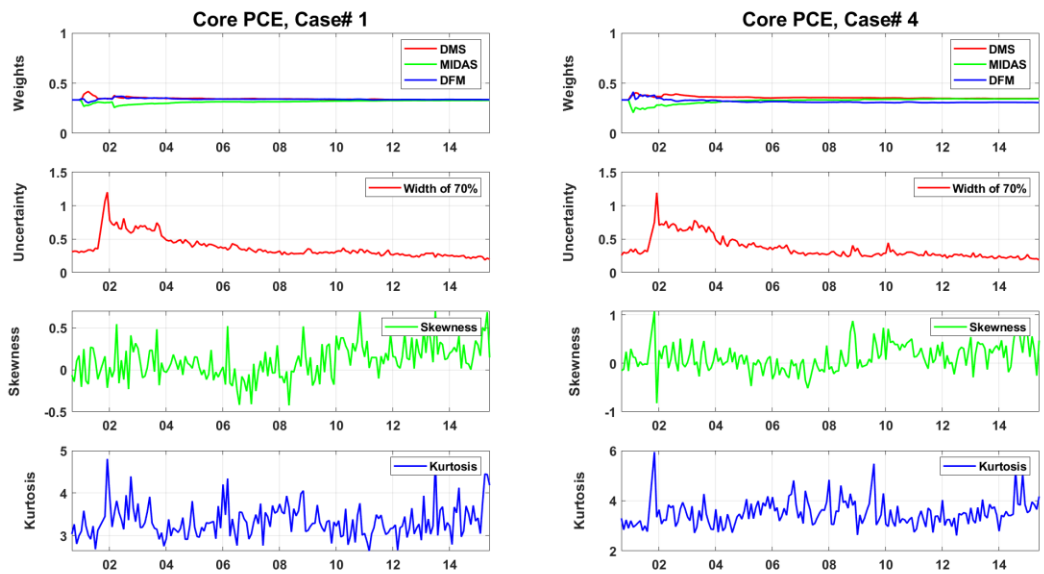

Notes: The first row of each panel plots the evolution of the weights for the three model classes underlying the grand combination, based on the flexible aggregation strategy and the CRPS weighting scheme. (Each model class is a combination of multiple model specifications.) The second row plots estimates of dynamic uncertainty, defined as the width of the 70% prediction intervals. The last two rows plot time-varying estimates of skewness and kurtosis. The sample period spans September 2000 through June 2015.

Figure A18: Comparison of Weights within the DMS Model Class, Log Score Weighting Scheme vs. CMG Weighting Scheme

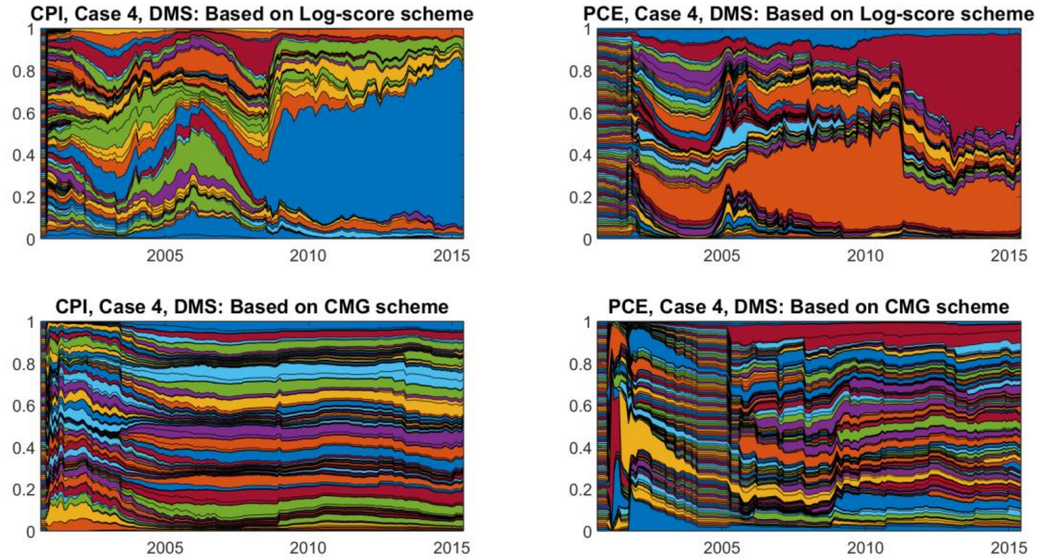

Notes: The figure plots the evolution of weights of the underlying individual candidate densities. Each color shade represents a particular individual candidate density. There are 108 candidate densities. The richness in the color variation indicates that no single candidate density dominates others. The left panel displays the weights for the stage 1 DMS combination constructed using the log score weighting scheme, and the right panel displays weights for the stage 1 DMS combination constructed using the CMG weighting scheme. The flexible aggregation method is used in both cases. The sample period spans September 2000 through June 2015.

Table A1 Representative Dates for Quarterly Nowcasting Performance

Case	Date	Information Set (Example: Nowcasting target quarter is Q1)	Months to Forecast
1	Last day of the previous quarter	December 31: Have CPI and PCE through November; high-frequency information through December 31	CPI: h=4 (Dec., Jan., Feb., Mar.) PCE: h=4 (Dec., Jan., Feb., Mar.)
2	Day 15 of month 1 of the target quarter	January 15: Receive CPI for December and have PCE through November; high-frequency information through end of second week of January, which includes two weekly retail gasoline readings from January	CPI: h=3 (Jan., Feb., Mar.) PCE: h=4 (Dec., Jan., Feb., Mar.)
3	Last day of month 1 of the target quarter	January 31: Have CPI for December and receive PCE for December; high-frequency information for all of January, which includes all four weekly retail gasoline readings from January	CPI: h=3 (Jan., Feb., Mar.) PCE: h=3 (Jan., Feb., Mar.)
4	Day 15 of month 2 of the target quarter	February 15: Receive CPI for January and have PCE through December; high-frequency information through end of second week of February, which includes two weekly retail gasoline readings from February	CPI: h=2 (Feb., Mar.) PCE: h=3 (Jan., Feb., Mar.)
5	Last day of month 2 of the target quarter	February 28: Have CPI for January and receive PCE for January; high-frequency information for all of February, which includes all four weekly retail gasoline readings from February	CPI: h=2 (Feb., Mar.) PCE: h=2 (Feb., Mar.)
6	Day 15 of month 3 of the target quarter	March 15: Receive CPI for February and have PCE through January; high-frequency information through end of second week of March, which includes two weekly retail gasoline readings from March	CPI: h=1 (Mar.) PCE: h=2 (Feb., Mar.)
7	Last day of month 3 of the target quarter	March 31: Have CPI for February and receive PCE for February; high-frequency information for all of March, which includes all four weekly retail gasoline readings from March	CPI: h=1 (Mar.) PCE: h=1 (Mar.)